Comparison of Integrated and Independent RF/FSO Transceivers on a Fading Optical Channel

Jonathan Nguyen, Ethan M. Liang, Linfang Wang, Richard D. Wesel
University of California, Los Angeles 90095
Department of Electrical and Computer Engineering
{nguyen.j,emliang,lfwang,wesel}@ucla.edu

Todd Drullinger, Todd Chauvin
SA Photonics
Los Gatos, California 95032
{t.drullinger,t.chauvin}@saphotonics.com

***Abstract*—Hybrid radio-frequency (RF) and free-space optical (FSO) transceivers harvest the high data rates possible with FSO while also maintaining a reliable link when clouds, fog, or dust interfere with the FSO channel. This paper compares two possible transceiver architectures: 1) an integrated RF/FSO modem with joint physical layer processing and 2) independent RF and FSO modems with separate physical layer processing assuming an intelligent router that multiplexes data to the two modems based on their time-varying throughput capabilities. While both architectures provide throughput benefits over a standalone FSO modem, the architecture featuring two independent modems demonstrates superior reliability under optical fading.**

I. Integrated and Independent Architectures.

Hybrid RF/FSO modems [1] harvest the high data rates possible with FSO while also maintaining a reliable link when clouds, fog, or dust interfere with the FSO channel. This paper compares a stand-alone FSO modem with both integrated and independent RF/FSO transceiver architectures. Fig. 1 shows the integrated architecture and Fig. 2 shows the independent architecture.

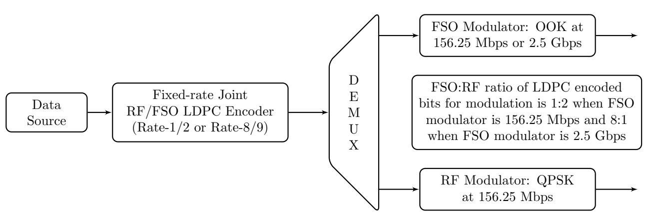

Fig. 1. Transmitter architecture for an integrated RF/FSO design where a single LDPC encoder provides coded bits to modulators for both the RF and FSO channels.

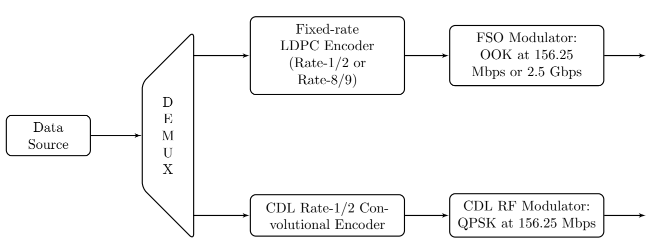

Fig. 2. Transmitter architecture for an independent RF/FSO design where independent encoders provide coded bits separately to modulators for the RF and FSO channels.

A fixed-rate protograph-based Raptor-like LDPC code [2] with rate-1/2 or rate-8/9 was used for the standalone FSO modem as well as the integrated RF/FSO architecture. For the independent architecture, the LDPC code was used for the FSO modem but the RF modem was assumed to be a legacy 64-state rate-1/2 convolutional code operating on a closed link.

The RF QPSK modulator transmits 156.25 megasymbols per second, thus modulating 312.5 megabits per second of convolutionally-coded or LDPC-coded bits. Two baud rates were considered for the FSO on-off keying (OOK) modulator, 156.25 megasymbols per second or 2.5 gigasymbols per second. Thus, the FSO OOK modulator modulates either 156.25 megabits per second or 2.5 gigabits per second of LDPC-coded bits, depending on the baud rate. Tables I and II summarize the throughput rates possible under the four configurations of FSO baud rate and LDPC code rate *assuming the links are closed.*

TABLE I
Overall data rates supported by the four configurations of the integrated RF/FSO modem assuming the link is closed.

	LDPC Rate 1/2	LDPC rate 8/9
FSO OOK 156.25 Megabaud	234.375 megabits per second	416.67 megabits per second
FSO OOK 2.5 Gigabaud	1.40625 gigabits per second	2.5 gigabits per second

TABLE II
Overall data rates supported by the four configurations of independent RF and FSO modems assuming all links are closed. The overall rates are lower than the integrated RF/FSO modem for the rate 8/9 LDPC code because the independent RF modem utilizes the legacy rate-1/2 convolutional code.

	LDPC Rate 1/2	LDPC rate 8/9
FSO OOK 156.25 Megabaud	234.375 megabits per second	295.14 megabits per second
FSO OOK 2.5 Gigabaud	1.40625 gigabits per second	2.376 gigabits per second

II. Channel Models

The RF channel model is QPSK in additive white Gaussian noise. The link is assumed to be closed for the legacy RF modem providing a data rate of 156.25 megabits per second. When the RF symbols are processed by the LDPC code in the integrated architecture, we explored performance when the E_s/N_0 was 4 dB and 7 dB. Following [3], our simulations use a Gaussian model for the avalanche photodiode detector.

According to this model each OOK slot contains either the signal or background noise, where both the signal and the background noise are modeled with Gaussian distributions. When the signal is present, the mean is μ_s and the variance is σ_s^2. When the signal is not present, the background noise has mean μ_b and the variance is σ_b^2. The bit log likelihood ratios from OOK used by the LDPC decoder are computed as

$$\lambda = \frac{1}{2} \ln \frac{\sigma_b^2}{\sigma_s^2} + \frac{(y-\mu_b)^2}{2\sigma_b^2} - \frac{(y-\mu_s)^2}{2\sigma_s^2} . \quad (1)$$

The fading behavior is slow with respect to a codeword length allowing a block fading model for simulation following [4]. The model generates a sequence of independent numbers according to a Gaussian distribution with zero mean and variance of ${\sigma_L}^2 = \log(PSI + 1)$. PSI is the Power Scintillation Index and describes how deep fade scintillations are. Next, these samples are passed through a low pass filter with frequency response given below in order to correlate them in time.

$$H(f) = \sqrt{{\sigma_L}^2 \tau_0 \sqrt{\pi}} \exp\left[-\frac{1}{2}(\pi \tau_0 f)^2\right] \quad (2)$$

The variable τ_0 is called the turbulence coherence time and describes the time interval during which the fade characteristics change very little. Finally, the output of the low pass filter is passed through a non-linear transformation given below:

$$a_{T_i} = e^{\left(x_i - \sigma_L^2/2\right)} \quad (3)$$

Fades are generated at a rate according to the turbulence coherence time and interpolated to provide additional samples.

III. Selecting LDPC Rate to Maximize Throughput

Let g be the fading channel gain in dB and define $g_{1/2}$ and $g_{8/9}$ as the thresholds in channel gain at which the respective codes close the link. Let B be the rate at which coded bits are transmitted through the channel. For FSO OOK, this is the same as the baud rate and independent of the LDPC rate. The approximate throughput T for each of the two LDPC rates can be expressed as follows:

$$T_{\frac{1}{2}} \approx \frac{1}{2} \times B \times P\left(g > g_{1/2}\right) \quad (4)$$

$$T_{\frac{8}{9}} \approx \frac{8}{9} \times B \times P\left(g > g_{8/9}\right) \quad (5)$$

These equations reveal that $T_{\frac{8}{9}} > T_{\frac{1}{2}}$ whenever $\frac{P\left(g_{1/2} \le g \le g_{8/9}\right)}{P\left(g > g_{8/9}\right)} < \frac{7}{9}$. Figure 3 shows the empirical probability mass function for each rate. Since each LDPC rate utilizes a different codeword length, they have different fading processes, but very similar histograms. For purposes of analysis, let us assume that $g_{8/9} = 0$ dB and $g_{1/2} = -3$ dB, which are consistent with our choice of baseline power on detector of -53.9 dB. For both histograms we can see that the empirical probability that a fade is in the left red box region $P\left(g_{1/2} \le g \le g_{8/9}\right)$ is about 0.1524 and the region in the right red box $P\left(g > g_{8/9}\right)$ is about 0.2227. Since $\frac{0.1524}{0.2227} = 0.6843 < 0.7778 = \frac{7}{9}$, the long-term average

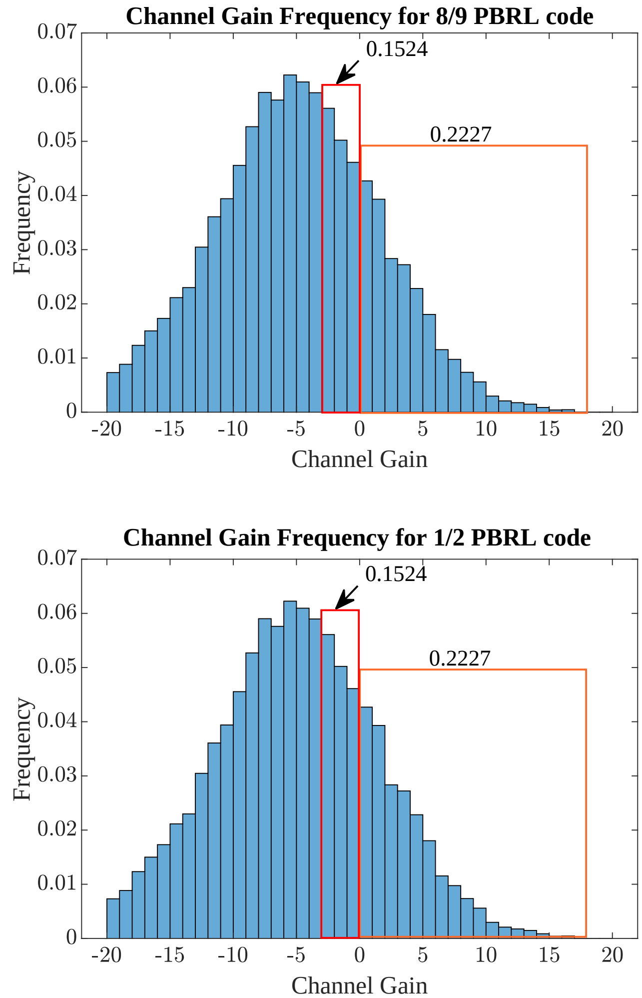

Fig. 3. Histogram of FSO channel fades taken over 10 seconds.

throughput would be optimized by the rate-8/9 LDPC code rather than the rate-1/2 LDPC code. Specifically, the rate-8/9 code would provide average throughput of 0.198 bits per FSO symbol while the rate-1/2 code would provide 0.1875 bits per symbol. The actual choice of LDPC coding rate would depend on the specific empirical PMF of fading gains, but the rule that $T_{\frac{8}{9}} > T_{\frac{1}{2}}$ whenever $\frac{P\left(g_{1/2} \le g \le g_{8/9}\right)}{P\left(g > g_{8/9}\right)} < \frac{7}{9}$ should guide the choice.

IV. Simulation Results and Conclusions

Figs. 4, 5,6, and 7 present the simulation results. The two architectures achieve similar throughputs in most scenarios. However, for the low baud rate (156.25 Mbps) FSO system, the 4 dB RF channel forced throughput to zero for the rate-8/9 integrated RF/FSO architecture. Independent RF and FSO modems provide good throughput in every scenario while also providing the advantage of maintaining a reliable RF link rather than losing all communication during the optical fades that cause link failure in the integrated architecture. The

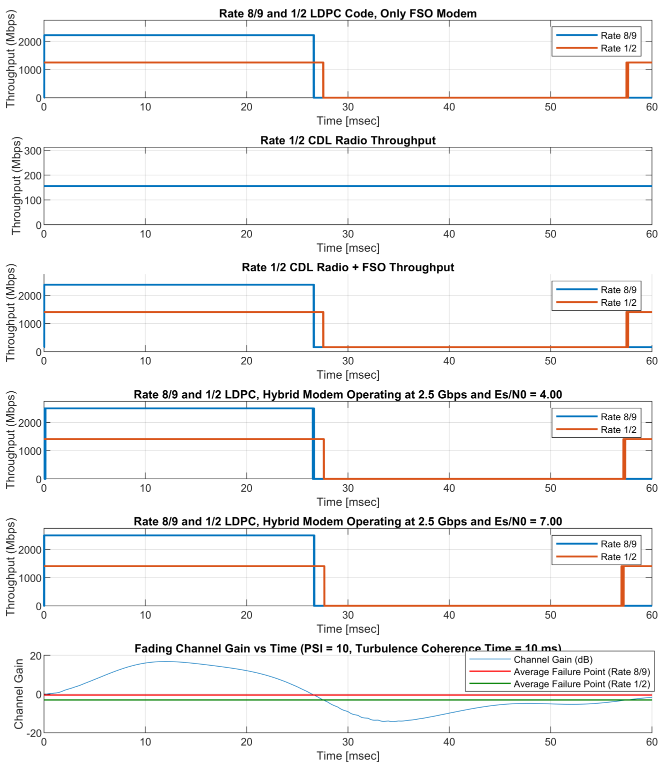

Fig. 4. Simulation results with FSO symbol rate is 2.5 gigasymbols per second showing the performance of independent RF and FSO modems and the integrated RF/FSO modem architecture on an optical fading channel (bottom plot). From the top, the first plot shows the instantaneous rate of the independent FSO modem for both rate-1/2 and rate-8/9 LDPC codes. The next plot shows the performance of the independent (CDL) modem on the RF channel. The third plot sums the previous two plots to provide the overall instantaneous rate of the two independent modems. The performance of the integrated RF/FSO modem architecture is shown in the fifth and sixth plots for RF channels with E_s/N_0 of 4 dB and 7 dB respectively.

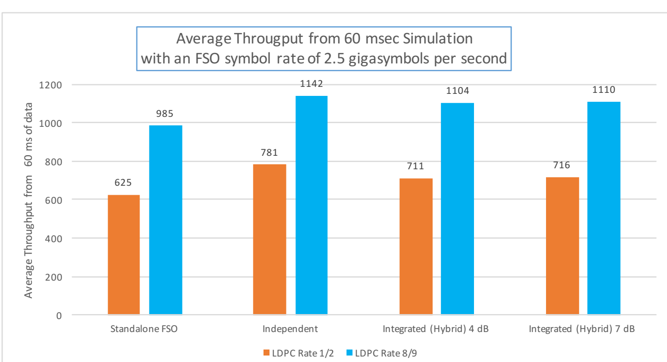

Fig. 5. Average throughput from 60 msec simulation for the various systems with the FSO symbol rate set to 2.5 gigasymbols per second.

essential throughput gain from utilizing both an RF and FSO channel can be obtained by deploying independent modems.

References

[1] M. N. Khan, S. O. Gilani, M. Jamil, A. Rafay, Q. Awais, B. A. Khawaja, M. Uzair, and A. W. Malik, "Maximizing throughput of hybrid fso-rf communication system: An algorithm,"

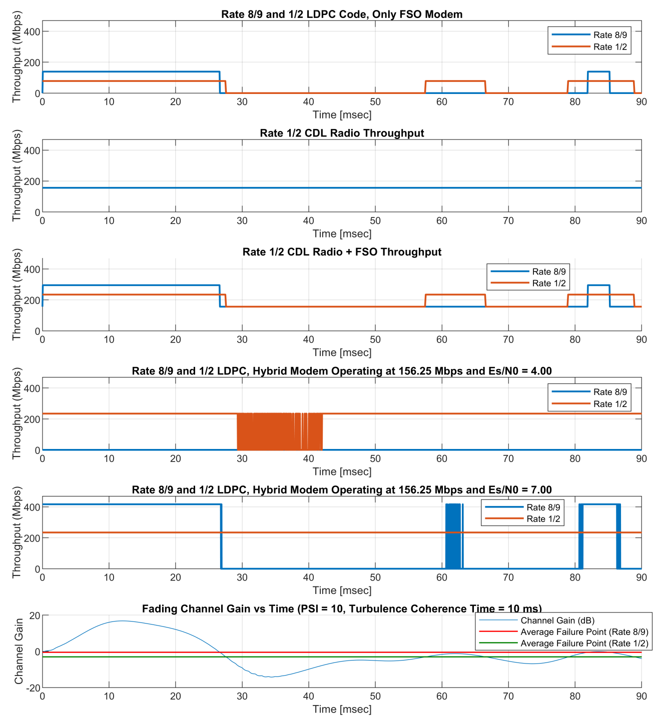

Fig. 6. Simulation results with FSO symbol rate is 156.25 megasymbols per second showing the performance of independent RF and FSO modems and the integrated RF/FSO modem architecture on an optical fading channel. Plot configuration is the same as Fig. 4.

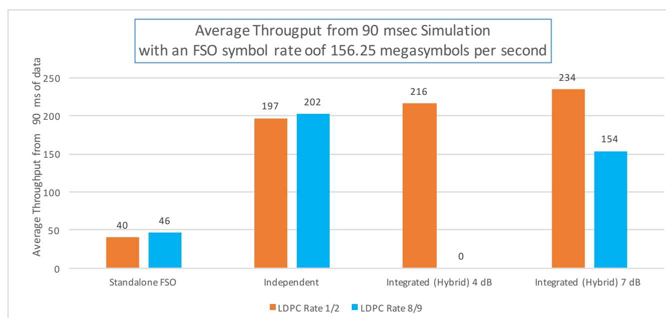

Fig. 7. Average throughput from 90 msec simulation for the various systems with the FSO symbol rate set to 156.25 megasymbols per second.

IEEE Access, vol. 6, pp. 30 039–30 048, 2018. [Online]. Available: http://dx.doi.org/10.1109/ACCESS.2018.2840535

[2] T.-Y. Chen, K. Vakilinia, D. Divsalar, and R. D. Wesel, "Protograph-based raptor-like ldpc codes," *IEEE Transactions on Communications*, vol. 63, no. 5, pp. 1522–1532, May 2015. [Online]. Available: http://dx.doi.org/10.1109/TCOMM.2015.2404842

[3] M. W. Wright, M. Srinivasan, and K. Wilson, "Improved optical communications performance using adaptive optics with an avalanche photodiode detector," Jet Propulsion Labroatory, California Institute of Technology, IPN Progress Report 42-161, 2005.

[4] Z. Kolka, "Channel model for monte-carlo simulation of data transmission on terrestrial fso paths," in *International Conference on Emerging Trends in Engineering and Technology*, 2013.